STATUS REPORT ON AN INVESTIGATION OF POWERED NACELLES ON A HIGH ASPECT RATIO NASA SUPERCRITICAL WING - PHASE II

Stuart G. Flechner, James C. Patterson, Jr., and Paul G. Fournier
NASA Langley Research Center

ABSTRACT

This is a status report on Phase II of an investigation of powered nacelles on a high aspect ratio NASA supercritical wing. Several separate flow and mixed flow nacelles were tested to determine the effect of nacelle and pylon cant angle variations and longitudinal and vertical position variations. Results are presented for the cruise condition: 0.82 Mach number and 0.55 lift coefficient.

INTRODUCTION

This is a status report on Phase II of the Langley propulsion/airframe integration investigation where several powered nacelles were installed on a proposed energy efficient transport having a high aspect ratio NASA supercritical wing and tested in the Langley 8-Foot Transonic Pressure Tunnel. The Phase I investigation compared short and long core separate flow nacelles, long duct and energy efficient engine (E^3) nacelles, symmetrical and cambered pylons, and several longitudinal and vertical nacelle locations. The Phase II investigation utilized a modified wing with the long core separate flow nacelle and several E^3 nacelles. The effects of nacelle and pylon cant angles and nacelle longitudinal and vertical location were investigated in detail. The investigation was conducted over a Mach number range from 0.70 to 0.83 although only the results at the cruise condition, 0.82 Mach number and 0.55 lift coefficient, are presented in this status report.

MODEL

Figure 1 shows a picture of the semispan model in the Langley 8-Foot Transonic Pressure Tunnel. The model was all-metric; that is, the fuselage was not attached to the tunnel sidewall. The fuselage was mounted on the balance which was located just outside the tunnel test section wall. Figure 2 is a dimensioned drawing of the model. The wing had a quarter chord sweep of 30°, an aspect ratio 10, and was 12 percent thick at the nacelle location which is 40 percent of the semispan.

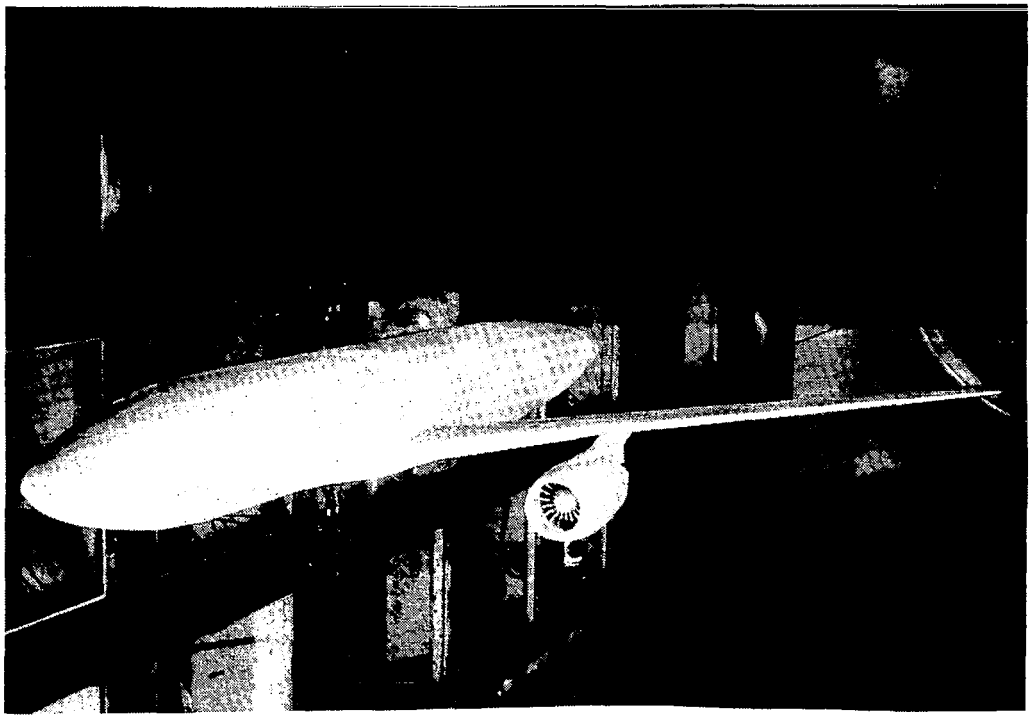

Figure 1

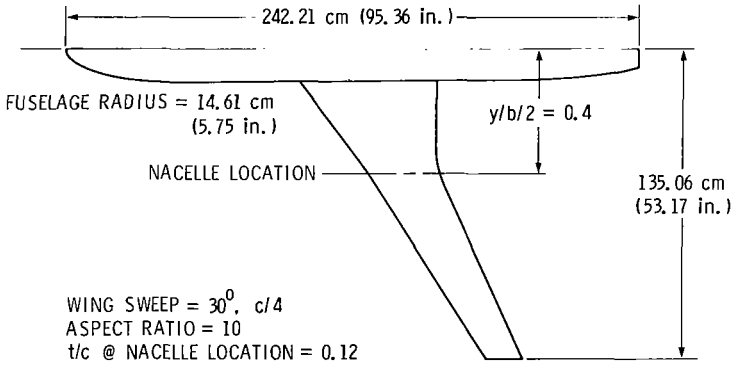

Figure 2

SCOPE OF PHASE II

The results obtained in Phase I indicated the changes required for the Phase II investigation. (See fig. 3.) A new outer wing panel was fabricated having 2.5° more wingtip washout and incorporating the latest modification to the supercritical airfoil section. These modifications consisted of a re-shaping of the lower surface of the airfoil section, at the engine location, near the leading edge and a reduction in the camber in the cusp region.

The wing-pylon attachment was also modified to provide a -2° nacelle "toe-in" capability for each nacelle pylon configuration and to reduce the nacelle incidence angle by 1°. Phase I results had indicated that a nacelle cant angle of -2° and a forward nacelle position was more desirable. Because of the increased wingtip washout, the cruise lift coefficient would be obtained at a higher angle of attack. Thus, the nacelle incidence angle was reduced 1° in an attempt to maintain the same nacelle alignment with the local flow.

SCOPE OF SECOND PHASE INVESTIGATION

- INCREASED WING TWIST
- WING LOWER SURFACE AIRFOIL RESHAPED
- NACELLE CANT OF -2 DEGREES (TOE-IN), Δ INCIDENCE -1°
- NACELLES IN FORWARD POSITION
- LIMITED TO LONG CORE AND E^3 NACELLES

Figure 3

EFFECT OF TWIST ON SPANWISE LOAD DISTRIBUTION

The effect of the increased wing twist on the spanwise load distribution for the wing fuselage configuration without pylons and nacelles is shown in figure 4. The data presented, at the cruise Mach number of 0.82 and at 2.5° angle of attack, are the normalized load at each spanwise wing station. The lift coefficient at this constant angle of attack was reduced by 0.02 due to the additional outboard twist. The loading on the outboard portion of the wing is reduced from the nacelle location to the wingtip as expected. In order to increase the lift coefficient of the new wing by this 0.02, an increase in angle of attack of approximately 0.3° was required.

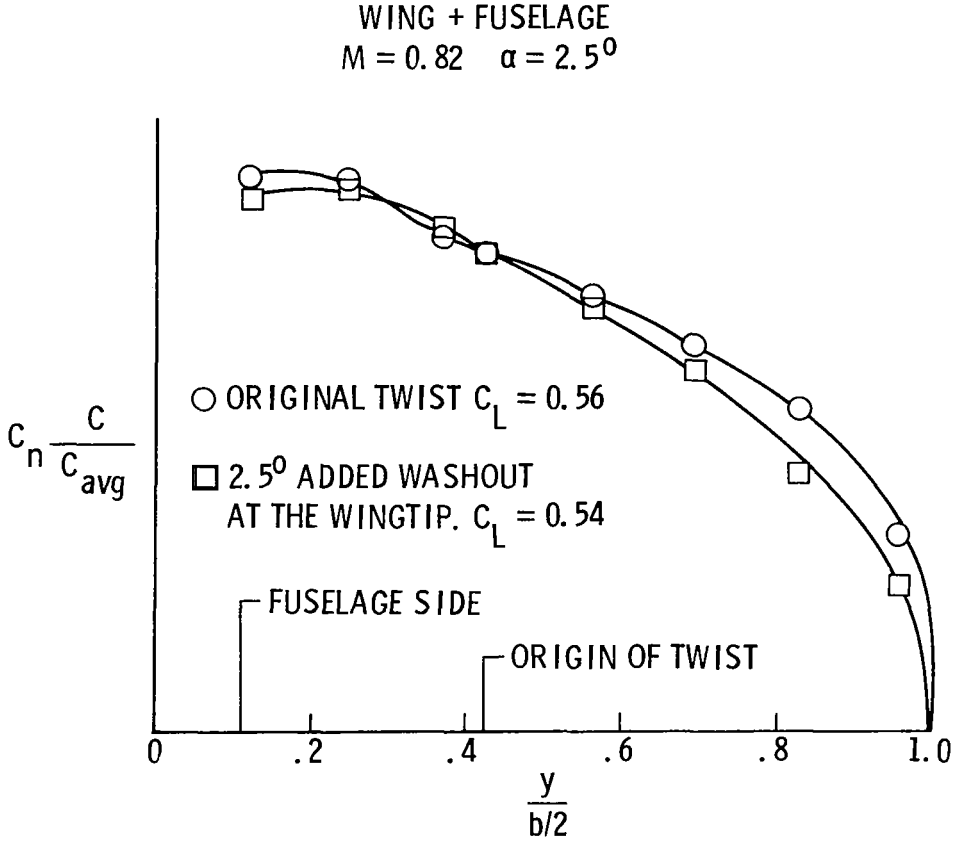

Figure 4

EFFECT OF AIRFOIL RESHAPING ON WING PRESSURE DISTRIBUTION

The chordwise pressure distribution measured just inboard of the nacelle location for the same configurations and conditions as for figure 4 is presented in figure 5. On the forward portion of the lower surface the velocities were reduced for the modified wing, as intended. On the upper surface of this airfoil section there are some changes that were not favorable as well as some that were. There is a stronger shock near the leading edge followed by a weaker shock at the 50 percent chord location followed again by an unfavorable shock recovery at the 70 percent chord location. While the causes of these differences have not yet been identified, several factors must be looked at. The airflow over the wing at this station was directly affected by the change to the lower surface shape near the leading edge and indirectly by the changes to the outboard wing panel. The new airfoil, incorporating the modified cusp and the start of the additional washout, starts just outboard of this station. The transition region between the airfoil shapes may have extended over the upper surface of this station. Accurate measurements of the wing will provide insight into the differences between the pressure distributions for the two phases.

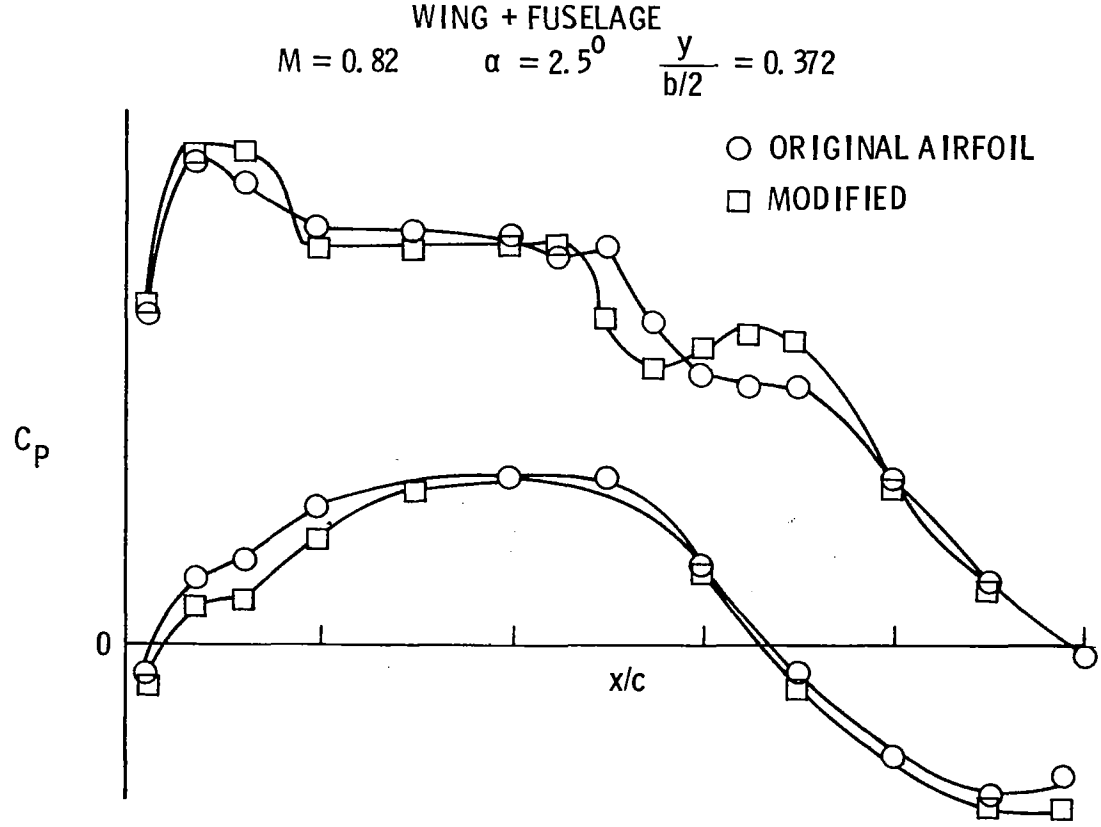

Figure 5

INCREMENTAL DRAG

The rest of this paper discusses the several powered nacelle configurations in terms of incremental drag (either installed drag or interference drag). Computing incremental drag requires testing four different configurations: the complete model; the wing and fuselage; the pylon and nacelle on an isolated strut; and the isolated strut alone. (See fig. 6.)

The installed drag is obtained by subtracting the drag of the wing fuselage configuration from the drag, adjusted for the calculated thrust, of the complete model configuration. The interference drag is obtained by subtracting the drag of the pylon and nacelle on the isolated strut, adjusted for the calculated thrust and the isolated strut tare, from the installed drag. A pylon and nacelle mounted on the isolated strut is shown in figure 7.

METHOD FOR DETERMINATION OF INCREMENTAL DRAG

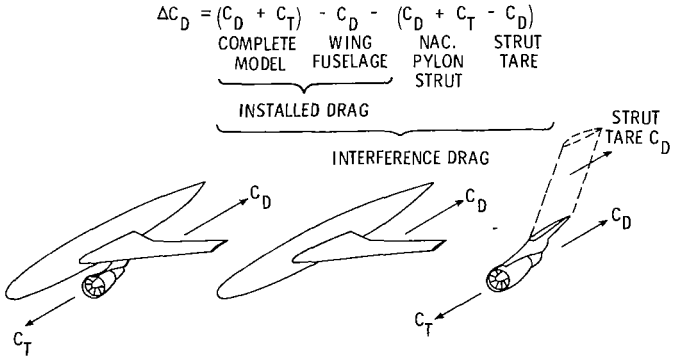

Figure 6

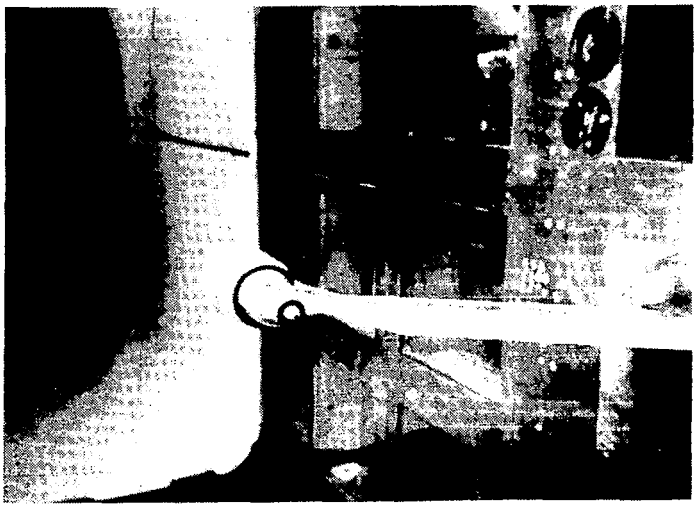

Figure 7

NACELLE CONFIGURATIONS

Figure 8 is a summary of the configurations that were investigated. The top two nacelles, the long core and the advanced E^3 nacelles were tested in Phase I as well as in this second test phase. The long core nacelle represents current technology; it is representative of the 50,000 pound thrust class engines. The advanced E^3, mixed flow nacelle represents advanced fan jet engine technology; at this time this engine is in the 37,000 pound thrust class which is expected to be increased to a thrust level comparable to that of the long core engine. The E^3 nacelle fan cowl has been extended to provide a more complete mixing of the fan and primary flows which has been shown to result in a 5 percent reduction in fuel consumption. This nacelle was tested in this second test phase. To compare separate and mixed flow nacelles effects, a separate flow nacelle comparable in size to the E^3 nacelle was also tested. This nacelle had a conical primary nacelle and plug.

Tests were conducted with different pylon and nacelle cant angles with the nacelles at several longitudinal and vertical positions. A sketch of the nacelle at a cant angle of -2° ("toe-in") is shown in figure 9 along with a view of nacelle position. The cambered pylon was tested at 0° and +2° cant angles. Phase I results indicate that there is a reduction in drag associated with the cambered pylon compared to the symmetrical pylon. The cambered pylons produce the desired side forces even at 0° cant angle. The nacelle's primary exit is located longitudinally with respect to the wing leading edge by the distance "X" (figure 9). The nacelle's centerline is located vertically with respect to the wing chord by distance "Z." The different nacelle configurations tested are presented in figure 10.

NACELLE CONFIGURATIONS

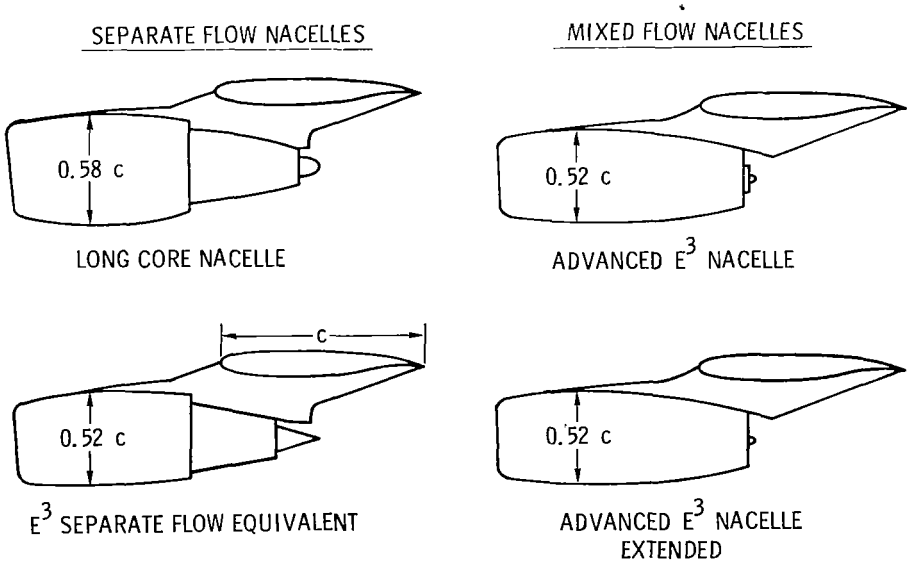

Figure 8

VARIATION OF ENGINE NACELLE POSITION AND ALIGNMENT

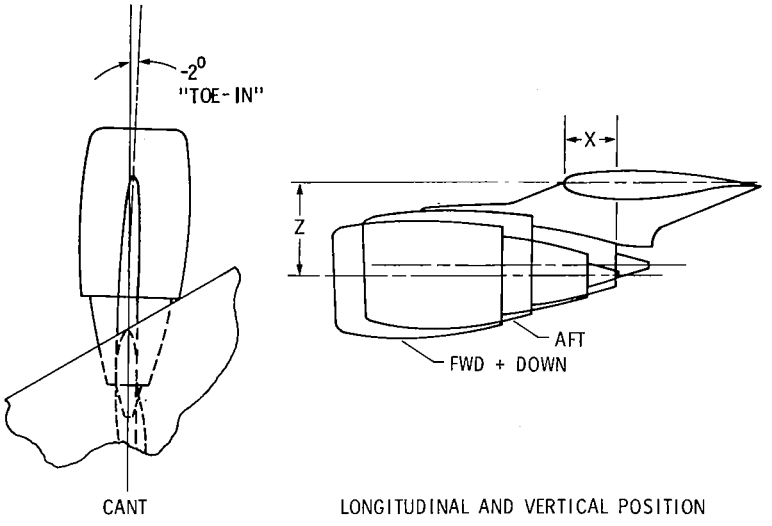

Figure 9

PROPULSION/AIRFRAME INTEGRATION INVESTIGATION

TEST CONFIGURATIONS

SEPARATE FLOW NACELLES

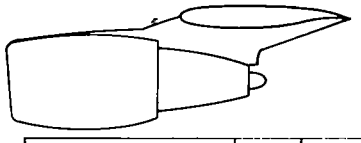

MIXED FLOW NACELLES

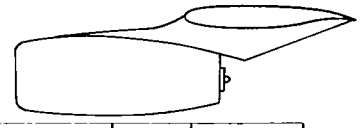

NACELLE CONFIG	PHASE	PYLON SHAPE		CANT ANGLE DEG		CORE EXIT	ENGINE CENTERLINE
		SYM	CAM	PYLON	NAC	LONGIT	VERTICAL
LONG CORE NAC (SEPARATE FLOW)	II		X	0	0	.40c	.40c
	II		X	0	-2	.40c	.40c
	II		X	0	-2	.25c	.45c
	II		X	0	-4	.40c	.40c
	II		X	+2	0	.40c	.40c
	II		X	+2	-2	.40c	.40c
E^3 CONICAL CORE NAC (SEPARATE FLOW)	II		X	0	-2	.29c	.40c
E^3 NAC (MIXED FLOW)	II		X	0	-2	.17c	.40c
	II		X	0	-2	.17c	.45c
	II		X	0	-2	.27c	.40c
	II		X	+2	0	.27c	.40c
E^3 EXTENDED NAC (MIXED FLOW)	II		X	0	-2	.29c	.40c

Figure 10

EFFECT OF LONG CORE NACELLE AND PYLON CANT

The effect of the nacelle and pylon cant angle variations on interference drag for the long core separate flow nacelle is presented in figure 11. Lower interference drag was obtained with a nacelle cant angle of -2° than with either 0° or -4° cant angles. The pylon cant angle of 0° in combination with the nacelle cant angle of -2° was shown to be more favorable than the +2° pylon cant angle.

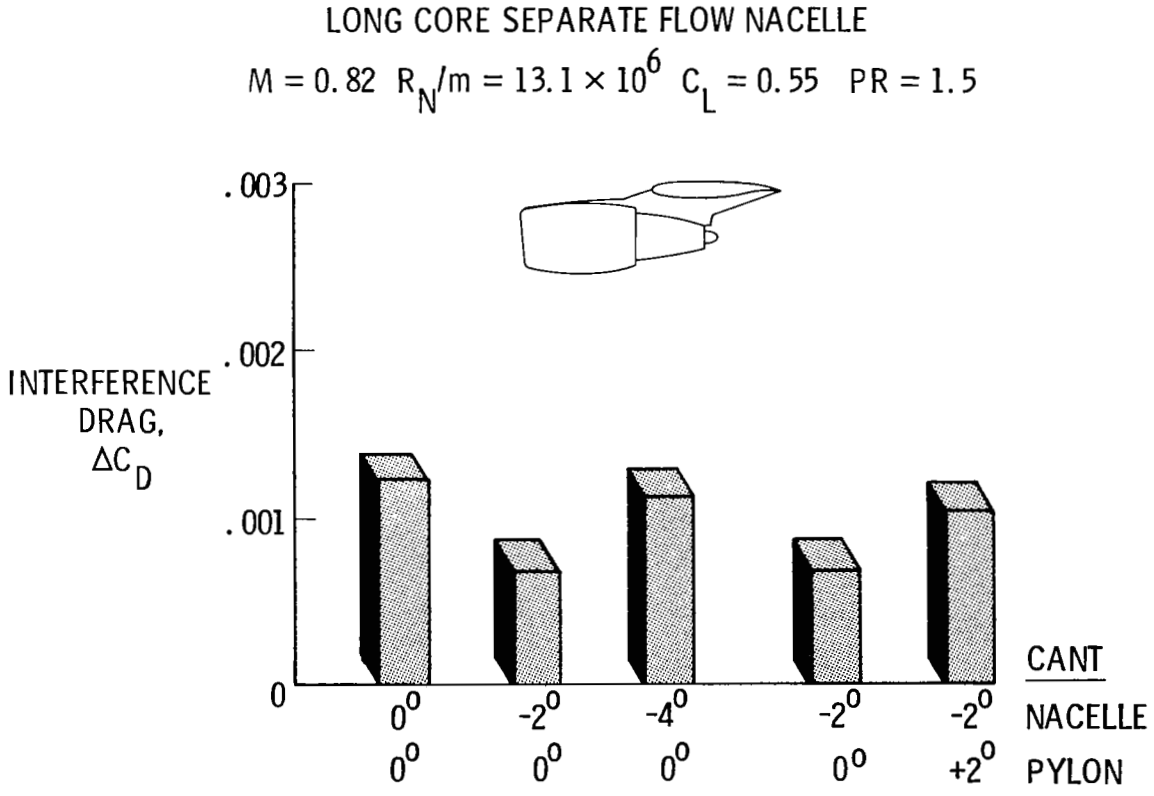

Figure 11

EFFECT OF LONG CORE NACELLE CANT ON PRESSURE DISTRIBUTION

The chordwise pressure distribution for the wing station just inboard of the nacelle is presented in figure 12. The -2° nacelle cant angle configuration has significantly lower velocities on the lower surface than either the 0° or -4° configurations. The 0° nacelle cant angle configuration also has a significant loss in lift at this station. The upper surface pressures near the wing trailing edge indicate there is some separation for the 0° nacelle cant configuration compared to that of the -2° or -4° configurations.

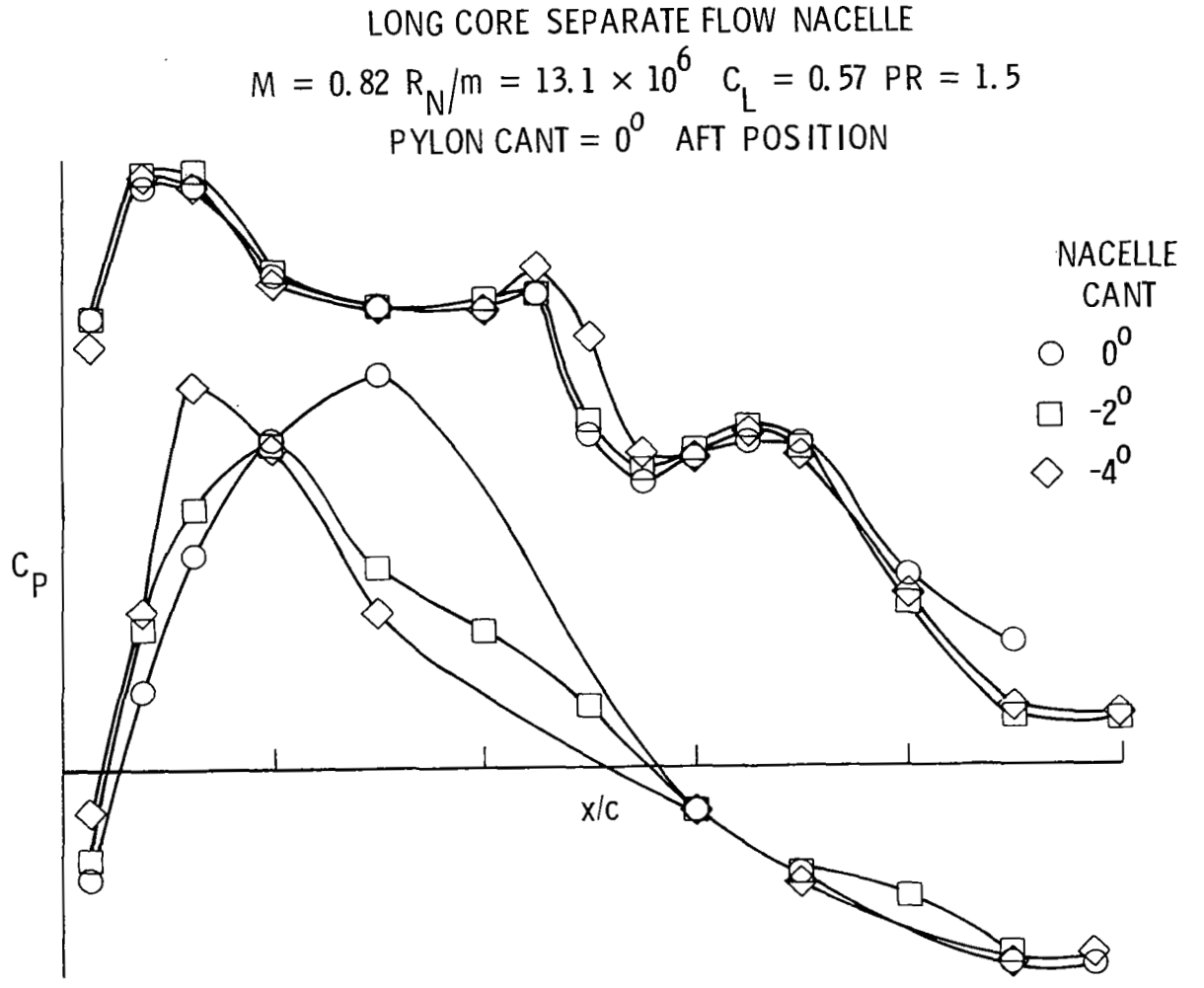

Figure 12

EFFECT OF LONG CORE NACELLE POSITION

Figure 13 presents the effect of the nacelle position on interference drag. Moving the nacelle from the aft position to the forward and down position resulted in an unexpected increase in interference drag. Results from previous powered nacelle tests had indicated that a forward position was more favorable than an aft position. A pylon was not available to produce a forward but not down position.

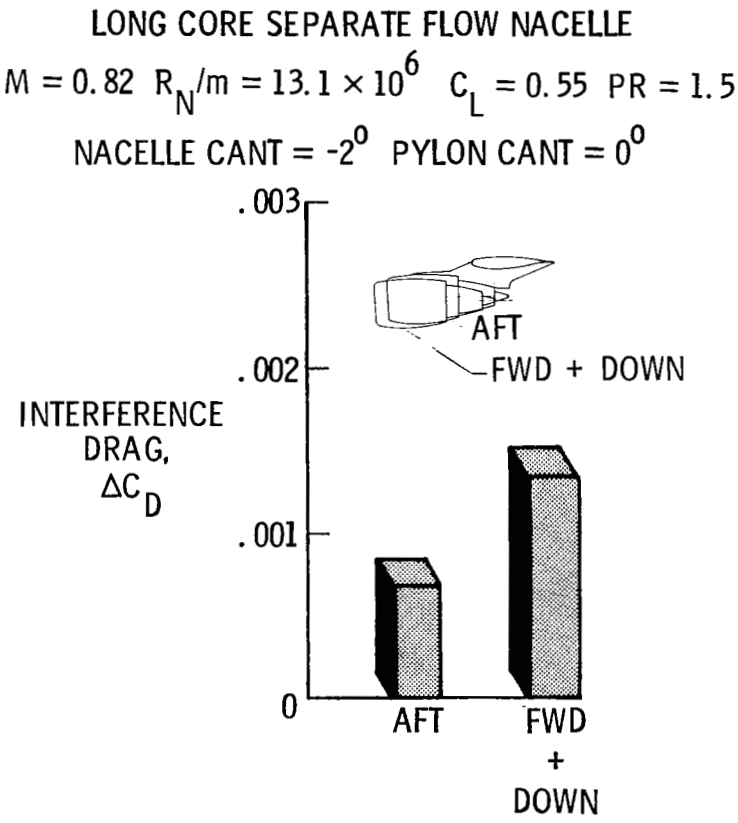

Figure 13

EFFECT OF E^3 NACELLE POSITION AND CANT

Figure 14 shows the effect of position and cant of the E^3 mixed flow nacelle. The forward position, as expected from Phase I results, had lower interference drag than either the aft or forward and down positions. These three positions were at the -2° nacelle cant angle and 0° pylon cant angle. The last two data columns show that the -2° nacelle cant angle and the 0° pylon cant configuration has less drag than the 0° nacelle cant and 2° pylon cant configuration. Again, there was no pylon available to test the intermediate configuration.

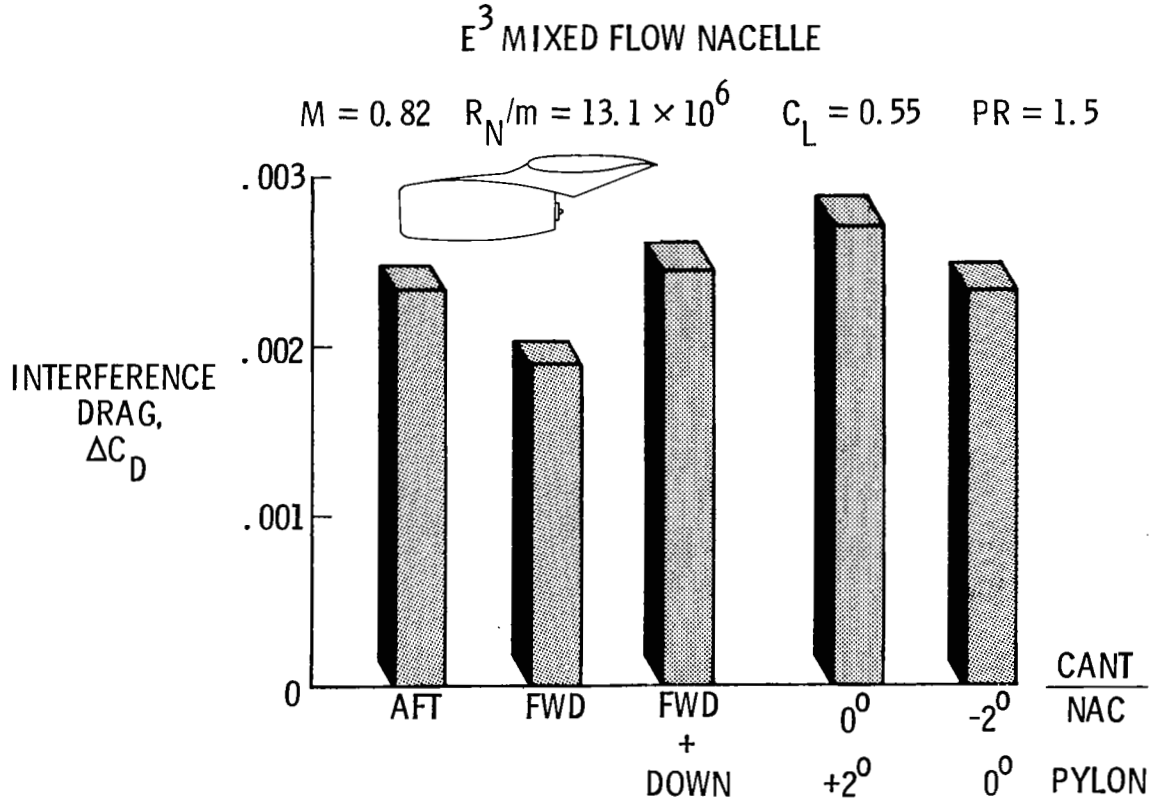

Figure 14

EFFECT OF E^3 NACELLE POSITION ON PRESSURE DISTRIBUTION

The pressure distribution over the wing chord just inboard of the nacelle, presented in figure 15, indicates the effects of nacelle position. The pressures on the wing lower surface for the aft position indicate a significant lift loss. The peak pressures along the lower surface are not very different for the three configurations although the two forward positions probably have a shock wave near the leading edge. The upper surface pressures indicate that the aft configuration has a lift loss over the rear portion but a lift gain over the forward portion of the wing. Near the trailing edge there probably is some separation with the forward and down position having a little more separation than either the aft or forward positions.

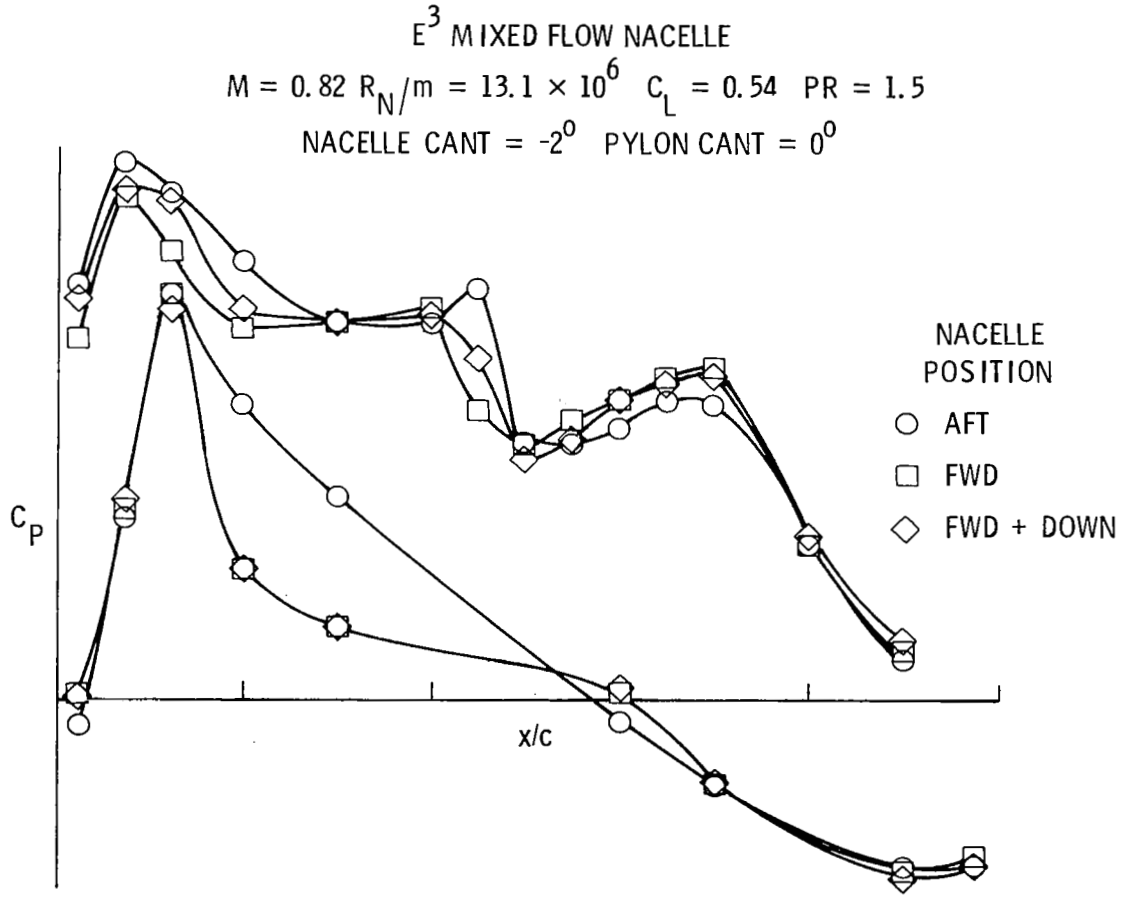

Figure 15

SUMMARY OF E^3 NACELLE TYPES

Figure 16 compares the several E^3 nacelle configurations, each with -2° nacelle cant, 0° pylon cant, and in the aft position. The results with the nacelle in the forward position are presented as the thin data column attached to the wider aft position column. The mixed flow configuration was improved, as expected, by going to an extended mixed flow configuration, but the separate flow configuration is still a better configuration than either mixed flow configuration.

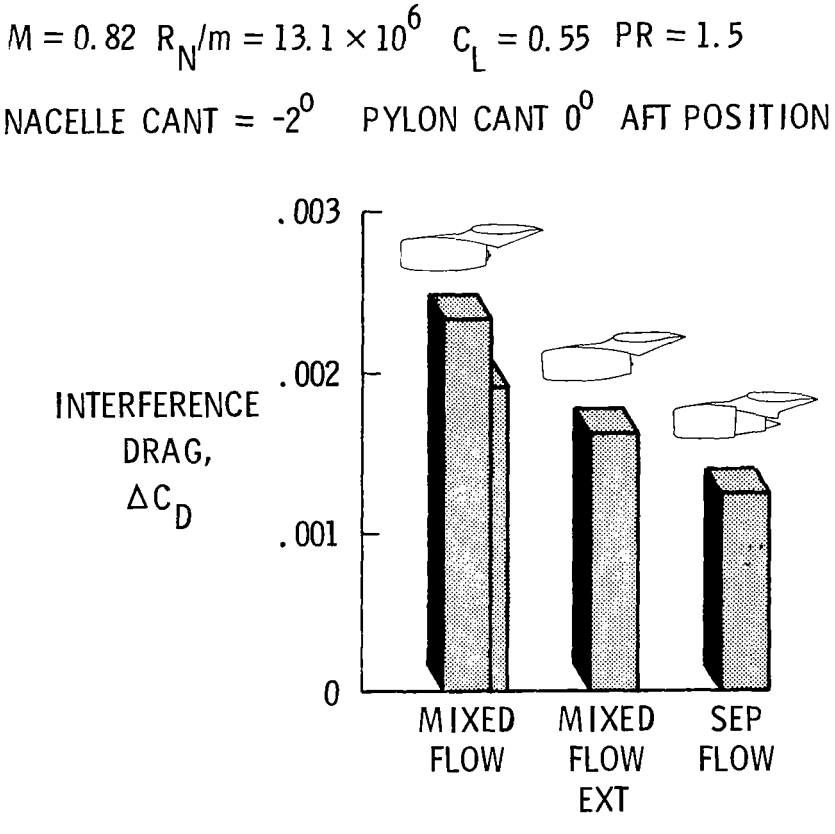

Figure 16

EFFECT OF E^3 FLOW-THROUGH NACELLE POSITION

Figure 17 shows the effect of the nacelle position for an E^3 flow-through nacelle. The nacelle has the same external shape as the E^3 mixed flow nacelle. The internal duct diameter decreased linearly from the inlet to the exit. Again, the forward position is better than either the aft or the aft and up position.

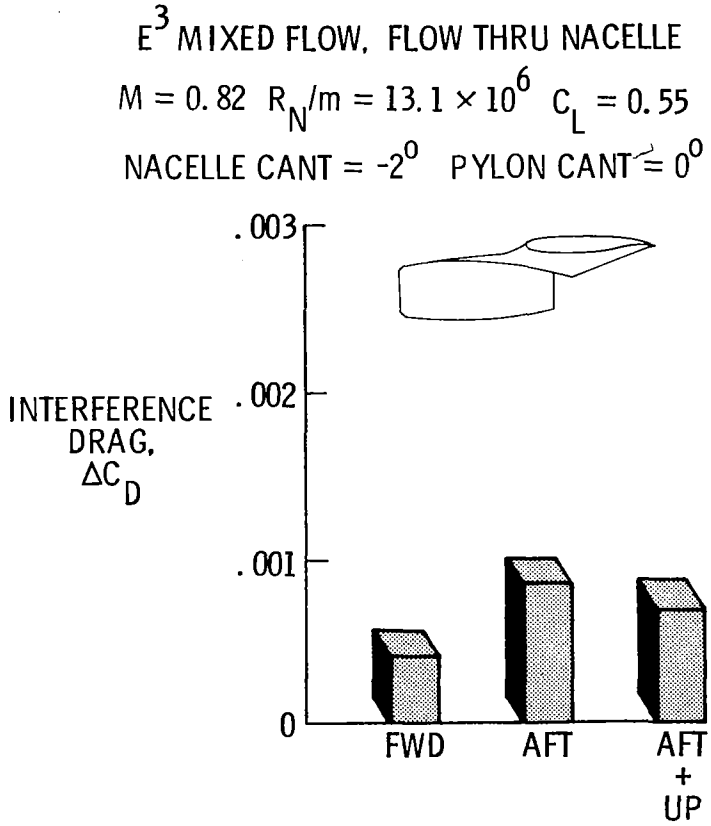

Figure 17

SUMMARY OF NACELLE TYPES

Both the installed drag, the drag of the complete model less the drag of the wing plus fuselage, and the interference drag, the installed drag less the drag of the engine-pylon configuration, are presented, for each nacelle tested, in figure 18. Each configuration has the same nacelle and pylon cant angles, -2° and 0°, respectively, and the data presented is for the nacelles in the aft position. In two cases the results obtained with the nacelles in the forward position are presented as thin data columns attached to the wider aft position columns. A comparison of the relative drag penalty associated with the installation of the various nacelles may be seen as well as that portion of the installation drag that is due to interference.

These data indicate that the long core separate flow nacelle has the lowest installation drag, with less intereference drag than the other powered nacelle configurations tested, even though the nacelle length and frontal area are somewhat greater. The longer primary core of this nacelle allows reduced boattail slopes resulting in reduced boattail drag. There may possibly be a favorable effect of the nacelle fan wake compared to the mixed flow nacelles that may also contribute to the lower drag of this configuration. The installation drag of the E^3 conical core separate flow nacelle is less than that of the mixed flow nacelle, half of which is interference drag. This is possibly a result of a reduction in the wing upper surface shock and reduced velocities associated with the separate flow nacelle on the forward portion of the wing lower surface, both inboard and outboard of the pylon. The extended mixed flow nacelle, extended for more complete mixing of the primary and fan flows, also is shown here to have a lower installation drag than the basic E^3 mixed flow nacelle. The thrust calibration of the basic E^3 nacelle has been in question and therefore it is planned to recalibrate this nacelle. It is conjectured, based on a similar circumstance, that the recalibration will result in a reduction in the installed drag coefficient of approximately 0.0004. This would reduce the drag level of the basic E^3 nacelle to just below the extended nacelle as would be expected.

The E^3 flow-through nacelle results are also presented on this figure, reduced by an internal drag coefficient of 0.00061. These data are compared with the basic E^3 nacelle and are shown to be approximately 30 percent less than the powered nacelle case. The installation and interference drag values for the flow-through and the E^3 powered nacelle in the forward position are also presented. In both cases there is a reduction in installation and interference drag in the forward position as shown in earlier powered nacelle investigations.

EFFECT OF NACELLE TYPE

$M = 0.82$ $R_N/m = 13.1 \times 10^6$ $C_L = 0.55$ PR = 1.5

INSTALLED DRAG = $\Delta C_D = C_D$ COMPLETE MODEL - C_D WING + FUSELAGE

INTERFERENCE DRAG = ΔC_D = INSTALLED DRAG - C_D ISOLATED NACELLE

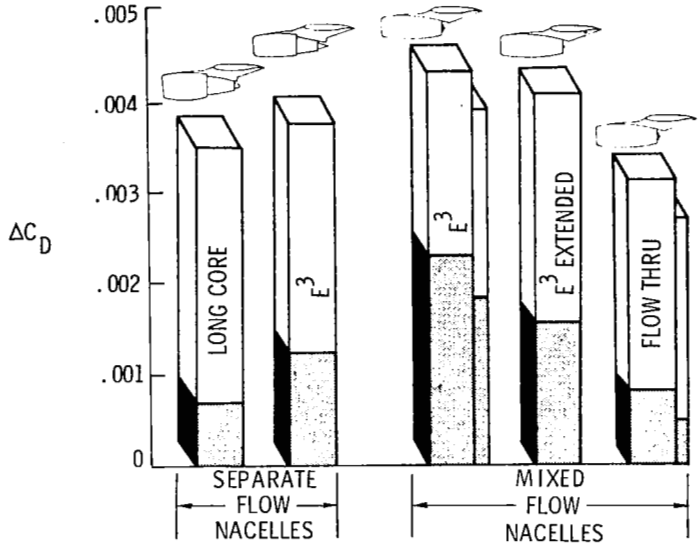

Figure 18

SUMMARY

The Phase II investigation was conducted with several separate flow and mixed flow nacelles. The effects of nacelle and pylon cant angle variations and longitudinal and vertical variations were investigated in detail. The results of the investigation, at the cruise condition, 0.82 Mach number and 0.55 lift coefficient, indicate that:

- Separate flow nacelles have less installation and interference drag than mixed flow nacelles
- Long core nacelles, representing current technology, have less installation and interference drag than the E^3 mixed flow and conical-core separate flow nacelles, representing advanced design technology.
- Best nacelle position and alignment:

  Forward position

  -2° nacelle cant angle ("toe-in")

  0° pylon cant angle